1 2 3 4 5 6 7 8 9 10 11 12 13 14 15 16 17 18 19 20 21 22 23 24 25 26 27 28 29 30 31 32 33 34 35 36 37 38 39 40 41 42 43 44 45 46 47 48 49 50 51 52 53 54 55 56 57 58 59 60

HCl Flow-induced Phase Change of α-, β- and ε-Ga_2O_3 Films Grown by MOCVD

Haiding Sun[1], Kuang-Hui Li[1], C. G. Torres. Castanedo[1], Serdal Okur[2], Gary S. Tompa[2**], Tom Salagaj[2], Sergei Lopatin[3], Alessandro Genovese[3], Xiaohang Li[1***]*

[1] King Abdullah University of Science and Technology (KAUST), Advanced Semiconductor Laboratory, Thuwal, 23955-6900, Saudi Arabia

[2] Structured Materials Industries, Inc., Piscataway, New Jersey 08854, USA

[3] King Abdullah University of Science and Technology (KAUST), Imaging and Characterization Core Laboratory, Thuwal 23955-6900, Saudi Arabia

KEYWORDS: epitaxial growth; gallium oxide (Ga_2O_3); MOCVD; phase change; HCl; wide band gap semiconductor;

ABSTRACT:

Precise control of the hetero-epitaxy on a low-cost foreign substrate is often the key to drive the success of fabricating semiconductor devices in scale when a large low-cost native substrate is not available. Here, we successfully synthesized three different phases of Ga_2O_3 (α, β, and ε) films on *c*-plane sapphire by only tuning the flow rate of HCl along with other precursors in an MOCVD reactor. A three-fold increase in the growth rate of pure β-Ga_2O_3 was achieved by introducing only 5 sccm of HCl flow. With continuously increased HCl flow, a mixture of β- and ε-Ga_2O_3 was observed, until the Ga_2O_3 film transformed completely to a pure ε-Ga_2O_3 with a smooth surface and the highest growth rate (~1 μm/hour) at a flow rate of 30 sccm. At 60 sccm, we found that the film tended to have a mixture of α- and ε-Ga_2O_3 with a dominant α-Ga_2O_3, while the growth rate dropped significantly (~0.4 μm/hour). The film became rough as a result of the mixture phases since the growth rate of ε-Ga_2O_3 is much higher than α-Ga_2O_3. In this HCl-enhanced MOCVD mode, the Cl impurity concentration was almost identical among the investigated samples. Based on our density functional theory calculation, we found that the relative energy between β-, ε-, and α-Ga_2O_3 became smaller thus inducing the phase change by increasing the HCl flow in the reactor. Thus, it is plausible that the HCl acted as a catalyst during

1
2
3
4
5
6
7
8
9
10
11
12
13
14
15
16
17
18
19
20
21
22
23
24
25
26
27
28
29
30
31
32
33
34
35
36
37
38
39
40
41
42
43
44
45
46
47
48
49
50
51
52
53
54
55
56
57
58
59
60

the phase transformation process. Furthermore, we revealed the microstructure and the epitaxial relationship between Ga_2O_3 with different phases and the *c*-plane sapphire substrates. Our HCl-enhanced MOCVD approach paves the way to achieving highly controllable hetero-epitaxy of Ga_2O_3 films with different phases for device applications.

INTRODUCTION

III-nitride semiconductor materials (AlN, InN, GaN, and their alloys) are of great interest due to their direct and wide bandgap that makes them suitable for power electronic and optoelectronic applications.[1,2,3] Remarkable breakthroughs have been achieved in the past decades. For example, (Al) GaN alloys have achieved a high critical electric field of ~3.5 MV/cm which makes it one of the best candidates for power electronics.[2] However, some semiconductor materials possess not covalent but ionic bonding. In this category, we can find wide band gap oxides of post-transitional metals that exhibit higher electrical breakdown strength, since higher electrical fields are needed to ionize charges. Among these oxides, Ga_2O_3 has attracted attention due to its extremely high theoretical breakdown field of ~8 MV/cm[4,5] which is even higher than SiC (3 MV/cm) and GaN (3.8 MV/cm). Over 1kV of reverse breakdown voltage in a vertical diode was achieved by using β-Ga_2O_3[6] and a record-high critical field strength of 3.8 MV/cm was reported in a homoepitaxially grown Ga_2O_3 MOSFET, already surpassing the GaN and SiC bulk theoretical field strengths.[7] In addition, due to its large intrinsic bandgap (4.5-5.1 eV), it is suitable for solar-blind deep ultraviolet (DUV) detection, and it can also be used as a UV-transparent template for other semiconductor materials.[8, 9] Furthermore, up to four-inch high-quality but costly native substrate produced by melt growth techniques are commercially available for large-scale device fabrication.[10] Additionally, Ga_2O_3 thin film can be doped with n-type dopant by different growth techniques such as halide vapor phase epitaxy (HVPE),[11] molecular beam epitaxy (MBE),[12] low-pressure chemical vapor deposition (LPCVD)[13] and metal-organic chemical vapor deposition (MOCVD)[14,15]; however, it has yet to be doped p-type.

Ga_2O_3 can form five different polymorphs designated as α, β, γ, δ and ε.[5,16,17] β-Ga_2O_3 is the most thermally stable one. This characteristic makes it possible to produce both single crystals and epitaxial β-Ga_2O_3 films. One approach for producing β-Ga_2O_3 epitaxial films is by vapor phase

epitaxy, for example by using trimethylgallium (TMGa) or triethylgallium (TEGa) and O_2 as precursors in a MOCVD[14,15] or by using gaseous $GaCl_3$ and O_2 in a HVPE reactor.[11] The main difference between these two techniques is that HVPE uses high Cl concentrations to produce very high growth rates. The β-Ga_2O_3 has a monoclinic structure, resulting in difficulty growing high-quality β-Ga_2O_3 films on hetero-substrates, i.e., sapphire and Si. Thus, the majority of existing β-Ga_2O_3-based power devices has been developed on expensive (-201) β-Ga_2O_3 native substrate.[6,7]

The ε-Ga_2O_3 was first synthesized by Roy et al. in 1952 using CVD[17] , but it was one of the meta-stable phases of Ga_2O_3 and transformed to β-phase at temperatures as low as 500 °C.[18,19] In contrast to β-Ga_2O_3, there are only a limited number of reports on the MOCVD-grown phase-pure ε-Ga_2O_3. Previously, most of the reported MOCVD-grown Ga_2O_3 has been grown above 550 °C, which results in the formation of β-phase only. Recently, Boschi et al. reported for the first time single-phase ε-Ga_2O_3 thin films grown on c-plane sapphire by MOCVD[20] and then later by Xia et al. on a less lattice-mismatch substrate of 6H-SiC.[19] Studies of successfully heteroepitaxial growth of metastable ε-Ga_2O_3 on sapphire mainly use HVPE technique which has fast growth rate (a few µm/hour). Researchers were able to achieve phase-pure ε-Ga_2O_3 on *c*-plane sapphire, GaN (0001), AlN (0001) and β-Ga_2O_3 (-201) by this technique at 550 °C.[21, 22] Since the ε-Ga_2O_3 is a highly symmetric hexagonal structure,[23,24] close to the III-nitrides, there is the implication that it should be possible to integrate ε-Ga_2O_3 with nitrides to form heterojunctions for optoelectronic devices. Thus, a precise control of the growth rate of ε-Ga_2O_3 by using MOCVD is necessary.

The α-Ga_2O_3 is another less-studied metastable phase of Ga_2O_3; it has corundum-like structure the same as α-Al_2O_3. Thus, α-Ga_2O_3 could be obtained on sapphire (α-Al_2O_3) substrate due to the similarity in lattice structure between the epilayer and the substrate.[25] However, most of the studies on the α-Ga_2O_3 grown on c-plane sapphire were demonstrated by using mist chemical vapor deposition (CVD)[26,27,28,29,30] and HVPE[31]. Pure MOCVD-grown α-Ga_2O_3 thin film on sapphire has not been reported to date. Nevertheless, study shows that three monolayers of pseudomorphic α-Ga_2O_3 can be stabilized by strain present at the interface between *c*-plane sapphire and β-Ga_2O_3[32], indicating α-Ga_2O_3 has a great potential to be used as novel buffer layers for epitaxial growth of other phases of Ga_2O_3 on sapphire. Additionally, α-Ga_2O_3 was

found to have the largest bandgap among all the forms of Ga_2O_3[33] and hence the highest electrical breakdown field compared with other phases.

In this study, we demonstrated for the first time, the successful growth tuning of three different phases of Ga_2O_3 in a MOCVD reactor by changing one growth parameter. Specifically, we introduced different flow rates of HCl gas along with constant Triethylgallium (TEGa) and O_2 precursors in the MOCVD reactor to precisely control the growth rate of Ga_2O_3 in *α-, β-* and *ε*-phases, superior to the other growth techniques such as HVPE and CVD. This is the first time to introduce HCl during oxides growth in a MOCVD reactor. We revealed the impact of HCl flow on the growth rate, phase transition, microstructures and optical bandgap of the investigated Ga_2O_3 samples. Further, we used density function theory to calculate the relative energy between different phases to find out how HCl flux can tune the phases of Ga_2O_3 and the calculation predictions are consistent with our experimental results. Now we are able to control the heteo-epitaxy growth of Ga_2O_3 precisely which is critical in the development of low-cost, large-scale Ga_2O_3-based devices for different applications.

EXPERIMENTS

All samples discussed in this paper were grown in an in-house vertical vapor phase epitaxy reactor at Structured Materials Industries, Inc. (SMI). The reactor consists of a 16-inch diameter stainless steel chamber and a single rotating disc reactor with a 13-inch platter. The gases flow from a showerhead at the top of the chamber. The sapphire substrates used in this work were single-side chemo-mechanically polished, 2-inch diameter and c-plane (001) unintentionally doped (UID). For the MOCVD growth runs, one hour each, the chamber pressure and temperature were maintained at 45 Torr and 600°C, respectively. Triethylgallium (TEGa) and O_2 were used as precursors and Ar as the carrier gas. Different HCl flows with 0, 5, 10, 30 and 60 sccm were introduced along with other precursors in different runs. Scanning electron microscopy (SEM) images were acquired using a Zeiss Merlin microscope under an acceleration voltage of 2 keV. Dimension Icon SPM atomic force microscopy (AFM) was used to study the surface morphology. The structural properties of these samples were examined by a Bruker D8 Advance X-ray diffractometer (XRD) using Cu Kα (λ=1.5405 Å) radiation. Depth profiling experiments were performed on a Dynamic (Secondary ion mass spectrometry) SIMS instrument from Hiden analytical company (Warrington-UK) operated at 10^{-9} Torr. A continuous Ar^+ beam

1
2
3
4
5
6
7
8
9
10
11
12
13
14
15
16
17
18
19
20
21
22
23
24
25
26
27
28
29
30
31
32
33
34
35
36
37
38
39
40
41
42
43
44
45
46
47
48
49
50
51
52
53
54
55
56
57
58
59
60

of 3 keV energy was employed to sputter the surface while the selected ions were sequentially collected using a MAXIM spectrometer equipped with a quadrupole analyzer. Micro- and nano-structures of Ga_2O_3 films were investigated using Thermofisher USA (former FEI) Titan Themis Z transmission electron microscope (TEM) equipped with a double Cs (spherical aberration) corrector. High-angle annular dark-field (HAADF) imaging has been performed in scanning TEM (STEM) mode using an acceleration voltage of 300 kV. Conventional TEM imaging and selected area electron diffraction (SAED) patterns were acquired using an FEI Titan ST microscope working at 300 keV. The thin TEM lamellae of the Ga_2O_3 samples were prepared via focused ion beam (FIB) milling by using an FEI Helios G4 FIB-SEM. All transmittance spectra were measured with a Shimadzu UV3600 spectrophotometer equipped with integrating sphere and baselined to Al mirror.

RESULTS AND DISCUSSION

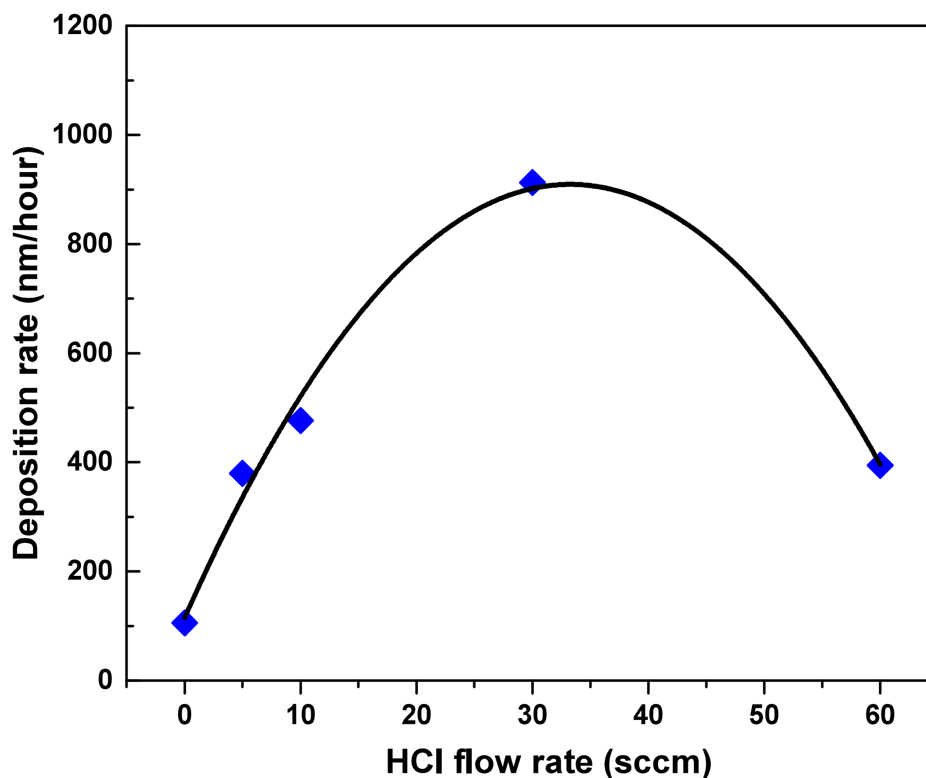

Figure 1. Growth rates of Ga_2O_3 films on c-plane sapphire substrates at various HCl flow rates (0, 5, 10, 30, 60 sccm).

1
2
3
4
5
6
7
8
9
10
11
12
13
14
15
16
17
18
19
20
21
22
23
24
25
26
27
28
29
30
31
32
33
34
35
36
37
38
39
40
41
42
43
44
45
46
47
48
49
50
51
52
53
54
55
56
57
58
59
60

The growth rates under different HCl flows were measured by using cross-sectional SEM. The growth rate exhibited a linear increase with increasing HCl flow rate, reaching the highest point of ~1μm per hour at 30 sccm. After this, the growth rate started to decrease with increasing the HCl flow and dropped to less than 300 nm per hour at 60 sccm, as shown in Figure 1. Therefore, the growth rate of Ga_2O_3 films can be controlled by carefully flowing HCl into the reactor along with the other precursors.

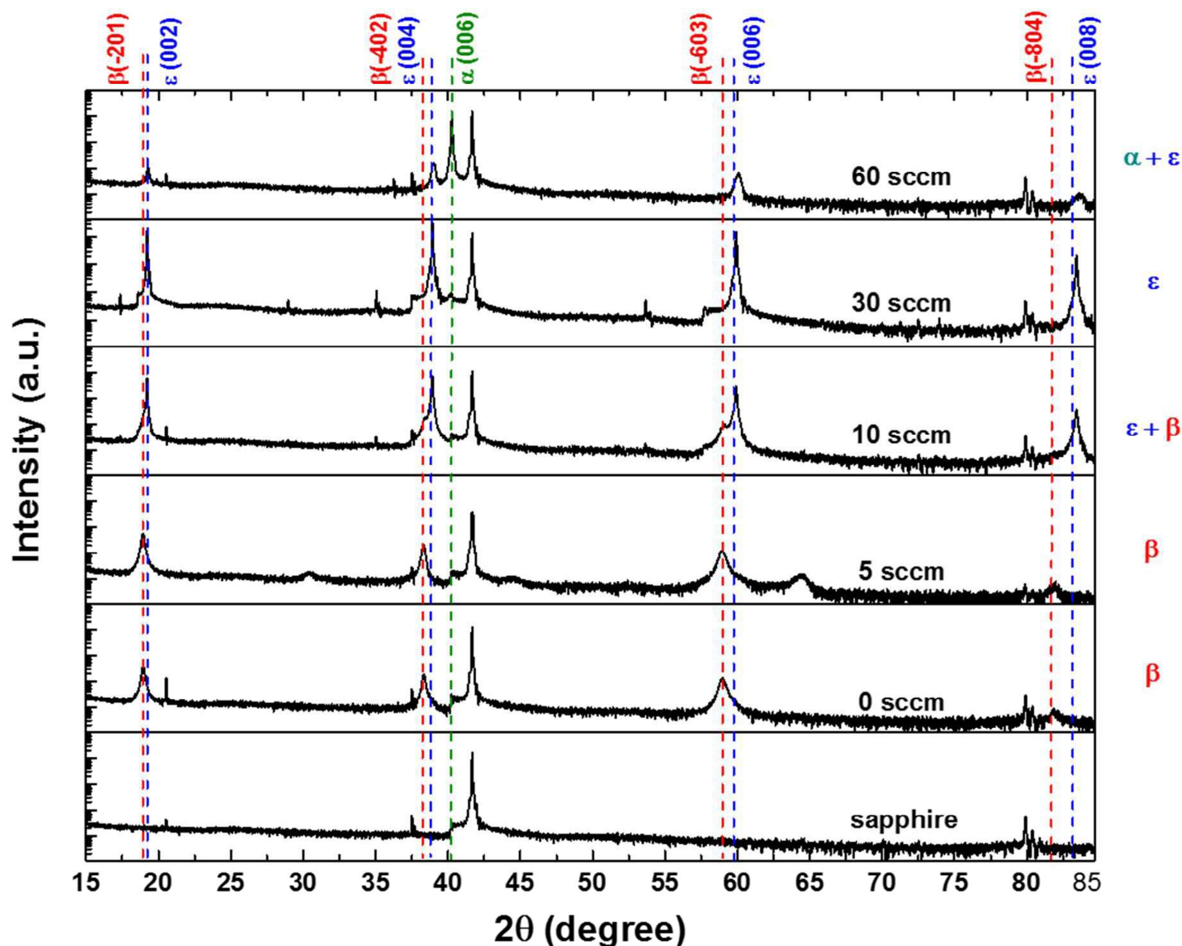

Figure 2. XRD patterns of Ga_2O_3 films grown under different flow rates of HCl.

1
2
3
4
5
6
7
8
9
10
11
12
13
14
15
16
17
18
19
20
21
22
23
24
25
26
27
28
29
30
31
32
33
34
35
36
37
38
39
40
41
42
43
44
45
46
47
48
49
50
51
52
53
54
55
56
57
58
59
60

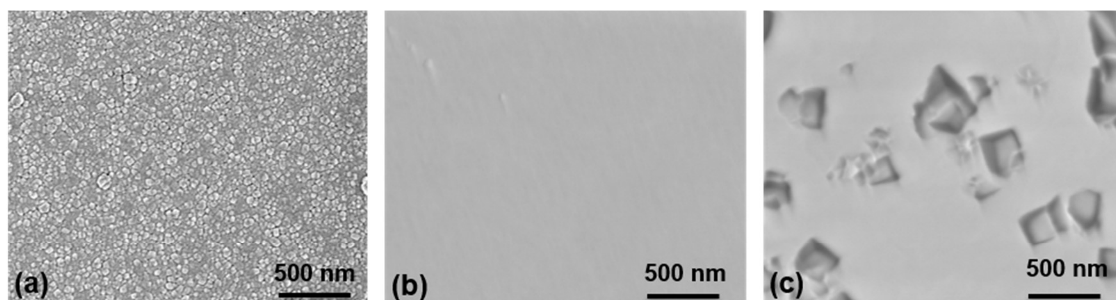

Figure 3. (a), (b), and (c) SEM images of the Ga_2O_3 films grown under 0, 30, 60 sccm of HCl.

Figure 2 presents the XRD patterns of Ga_2O_3 films grown at increasing HCl flow rates. For the growth without HCl flow, a phase-pure β-Ga_2O_3 film was obtained. The diffraction peaks at 18.96°, 38.38°, and 59.15° are assigned to the low and higher-order diffractions of β-Ga_2O_3. We can observe small β-Ga_2O_3 grain structures in this sample (as shown in Figure 3(a)). With introducing a flow rate of 5 sccm, we observe the same three peaks along with additional β-Ga_2O_3 peaks at 31.02° (-110) and 64.89° (-204). Upon keep increasing the HCl flow to 10 sccm, new diffraction peaks appeared at 19.23°, 38.93°, and 59.93° corresponding to 002, 004 and 006 diffractions of ε-Ga_2O_3, respectively. These results indicate that the Ga_2O_3 film transformed into a mixture of β- and ε-Ga_2O_3 and the growth rate continued to rise. At the flow rate of 30sccm, a phase-pure ε-Ga_2O_3, with only diffraction peaks at 19.23°, 38.93°, and 59.93°, was obtained. We measured the full-width at half-maximum (FWHM) of the rocking curve of the 006 diffraction peak of β-Ga_2O_3 without HCl flow (0.812°). This value was nearly two times larger than that of the ε-Ga_2O_3 (0.420°), implying that the crystal quality of ε-Ga_2O_3 was improved compared to β-Ga_2O_3 under such growth conditions. Consistent with the XRD results, an obvious improving in the surface morphology was observed. As displayed in Figure 3 (b), the phase-pure ε-Ga_2O_3 has a flat surface with surface roughness about 2.4 nm measured by AFM in a 1×1 µm scan area and it also has the highest growth rate among the investigated samples (Figure 1).[14] By further increasing the flow rate up to 60 sccm, a new diffraction peak appears at 40.15° which corresponds to the (006) reflection of α-Ga_2O_3, coexisting with other three main peaks from ε-Ga_2O_3 but with much lower peak intensity. Thus, the film has a dominant phase of α-Ga_2O_3. The FWHM of the rocking curve of the (006) peak of the α-Ga_2O_3 has the lowest value of 0.212°, among all these samples, indicating highest crystallinity. SEM image (Figure 3 (c)) indicates the film became rough due to the existence of mixture phases. A 3-dimensional (3D) grains are

visible on the surface clearly. Based on the results, the HCl flow variation changes not only the phases of Ga_2O_3 but also the growth rate and morphology of the films.

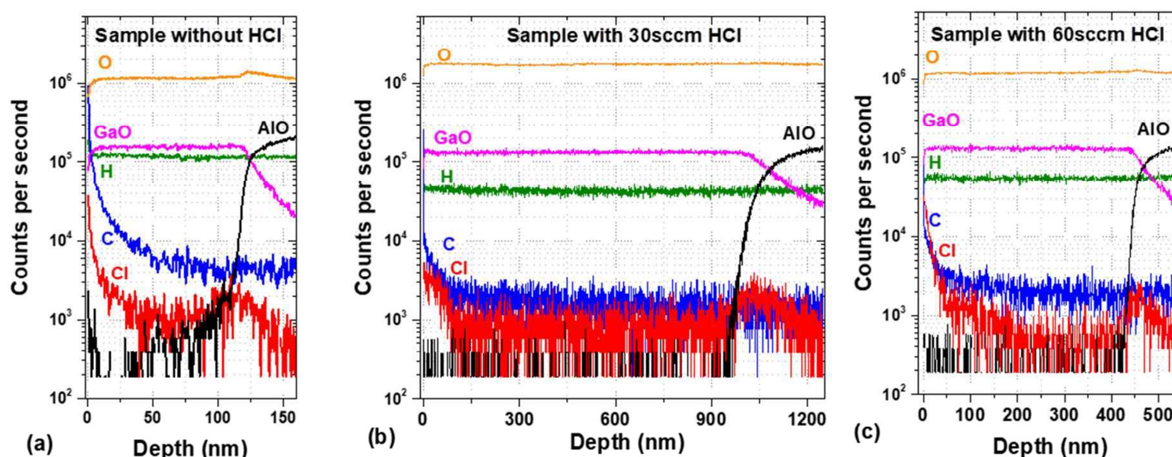

Figure 4. SIMS depth profiles of the Ga_2O_3 films with 0, 30 and 60 sccm flow rate of HCl.

Figure 4 shows the impurity depth profiles measured by SIMS for the samples with 0, 30 and 60 sccm flow rate of HCl. Compared with the concentration of "H" and "C" in the samples with 30 and 60 sccm flow of HCl, a higher concentration of both elements in the sample without HCl is observed, mainly attributed to its poorest crystal quality which often introduces additional impurities in MOCVD-grown materials. The largest value of FWHM of XRD rocking curve and very rough surface (shown in Figure 3(a)) with grain structures and columnar features were described earlier, indicating low crystallinity in this sample. The grainy surface could also enhance the impurity absorption. The Cl concentration in all the Ga_2O_3 film shows similar values, as well as its background level in the sapphire substrates. Normally, the Cl concentration can be detected in the HVPE-grown Ga_2O_3 film likely originating from the precursor, even though the concentration was quite low.[11] However, in our case, the HCl flow does not affect the Cl concentration in the films. We believe the HCl acts as a catalyst for the growth since it does not incorporate in Ga_2O_3 but actively evolves during the growth.

We performed density function theory (DFT) calculations (details in ESI) to verify and explore how HCl flux can tune the phases of Ga_2O_3 (detailed calculation can be found in supporting information Section S1). The growth of the crystal Ga_2O_3 is understood following the Ostwald's

description: the Ga_xO_y firstly forms nuclei, which is a rate-limiting step, where the thermodynamic factors control the whole process. After that, the reactants grow on the nuclei, and the kinetic factors may govern this process. Therefore, our calculation is based on the assumption that the nuclei may determine the morphology of the final product, and the calculations focus on the relative energies corresponding to the thermodynamic controlled process.

First, the relative energy corresponding to the α-, β-, ε-phases of Ga_2O_3 were calculated and listed in Table 1. Consistent with experiment, the β-phase Ga_2O_3 has the lowest energy, indicating without any modification, it can be the dominant product. This result matches the earlier studies in which they have also shown that the formation energy has the tendency of $\beta<\varepsilon<\alpha$ during the Ga_2O_3 synthesizing process which indicates that β-phases Ga_2O_3 should be the primary product after processing.[34,35,36] Then, we gradually doped the hydrogen atoms into the material to achieve the relatively hydrogenated Ga_4O_6H. The relative energies were calculated and listed in Table 1 as well. With the increment amount of doped hydrogen, the relative energy for epsilon phase is decreased, indicating epsilon phase material may be more favorable. This is consistent with experimental results, that the HCl flux may offer the hydrogen resource and produce more epsilon-phase material. Our hypothesis is as follows: since hydrogen is quite light and can leave the material by forming H_2O under reaction condition, the hydrogen may work as the catalysis to tune the structure. With further increment of the hydrogen resource, the relative energy between different phases is even smaller. Considering the precision of the DFT calculations and our model, the results may show the trend that doping hydrogen into the material can shift the relative energy of different phases of Ga_2O_3. However, our model may have simplified to explain the real reaction. Further studies regarding kinetic models may be required to unveil the whole mechanism of the crystallization process with HCl including: (1) fully understand the growth rate versus the HCl flow rates of Ga_2O_3 with the same phase. (2) Oversupply HCl gas into the chamber to check the phases and growth rate. (3) Replace HCl with other gas to conduct similar study etc. Nevertheless, in our case, as the HCl flow continues to rise, we suspect that the difference in free energy between the β, ε, and α becomes smaller due the involvement of HCl in the reaction. Eventually, the ε-phase becomes more stable and then the α-phase after flowing 30 and 60 sccm of the HCl gas, respectively.

Table 1. Relative energy different between different phases.

Type	Alpha	Beta	Epsilon
Relative Energy/Ga_2O_3 unit	0.15 eV	0.00 eV	0.04 eV
Relative Energy/Ga_4O_6H unit	0.07 eV	0.02 eV	0.00 eV
Relative Energy/$Ga_4O_6H_2$ unit	0.01 eV	0.03 eV	0.00 eV

In the following section, a detailed microstructure analysis was performed to investigate these films below.

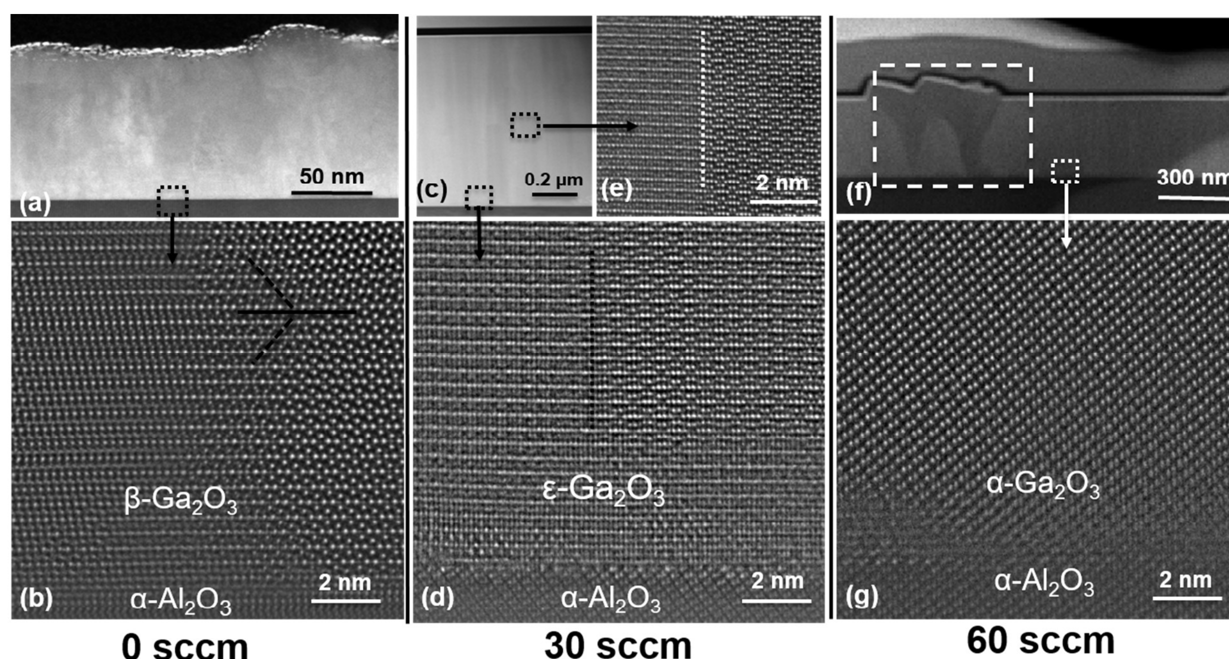

Figure 5. HAADF STEM imaging of FIB cross-section samples grown under HCl flow rates of 0, 30 and 60 sccm. (a), (c), (f) Low-intermediate magnification. (b), (d), (g) High magnification STEM images (Gaussian high-pass filtered image) collected at the interface of the three samples, respectively. (e) Detail at the domain boundary along the film.

Cross-sectional HAADF STEM images show three distinct nano-structures due to different HCl flow. In the film without HCl flow, we observe a columnar shape of β-Ga_2O_3 along the growth direction, indicating a columnar growth mode which might lead to a rough surface, as shown in Figure 5 (a). The contact between the β-Ga_2O_3 film and sapphire substrate exhibits epitaxial

1
2
3 relationships generally, with the β-Ga_2O_3 [-201] crystal direction parallel to the sapphire [0001] crystal direction. In particular, the β-Ga_2O_3 film displays a nano-domain structure including twining structures as well (marked in black dash line in (b)). Due to the large lattice mismatch between (-201) β-Ga_2O_3 and c-plane sapphire, inevitably, disoriented domains can form during the growth process. The sample grown with HCl flow rate of 30 sccm shows a flat top with pure-phase ε-Ga_2O_3 (Figure 5 (c)). However, we observe two domains nucleated at the ε-Ga_2O_3/sapphire interface with a sharp vertical boundary (marked by the black dash line in Figure 5 (d)). Unlike the intermixing texture between different crystal domains in the β-Ga_2O_3, the domains in ε-Ga_2O_3 are highly aligned and well-maintained along the growth direction, as confirmed by the high-resolution STEM (HR-STEM) imaging performed far away from the interface (Figure 5(e)). We observe an alternated texture of the domains in the pure-phase ε-Ga_2O_3, marked by white dash line. The detailed analysis of the pure-phase ε-Ga_2O_3 is carried out and discussed in the supporting information Section S2. Figure 5(f) shows a smooth film although some three-dimensional (3D) grains can be observed on the surface. The growth rate of the film was estimated to be approximately 0.4 μm/h. As can be seen in Figure 5(f), these are originated at the interface with the substrate as seen in color contrast between the 3D grains with the rest of the flat film; thus, their surface density is independent of the growth time. We collected HR-STEM images at the interface with a flat surface. The α-Ga_2O_3 exhibits a clear epitaxial growth over the sapphire substrate. The corresponding symmetry relationships are determined to be [10-10] α-Ga_2O_3 ‖ [10-10] sapphire, indicating that α-Ga_2O_3 has a uniform growth rate thus flat surface, as shown in Figure 5(h). The crystal structure of the 3D-grains will be elaborated below.

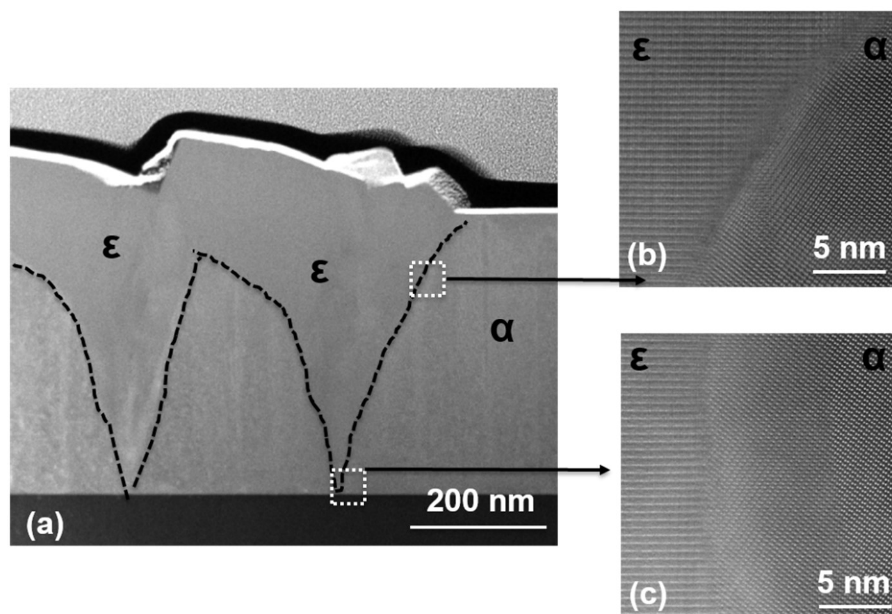

Figure 6. HADFF-STEM observation showing the structural evolution of the mixed-phase sample (α- and ε-Ga_2O_3) during the film growth. (a) An overview of the 3D grains marked in white dash square in Fig 5(f). The top (b) and the bottom (c) part of the 3D grains.

Figure 6 (a) shows the evolving of the 3D-grains during the film growth. As the 3D-grains grew laterally and vertically faster than the rest of epilayers (the growth rate of ε-Ga_2O_3 is larger than α-Ga_2O_3[22]), the grain-size increased continuously, becoming more protruding with the growth time as observed in the bottom and the top part at the boundary between the α- and ε-Ga_2O_3 (Figure 6 (b) and (c)). To avoid the formation of such 3D-grains embedded in the α-Ga_2O_3 film matrix, it is necessary to improve the growth conditions at the early growth stage, during the nucleation, in order to suppress the formation of the 3D-grains. HRTEM and FT analysis of the interface region in sample grown with 60 sccm of HCl flow rate are presented in supporting information Section S3.

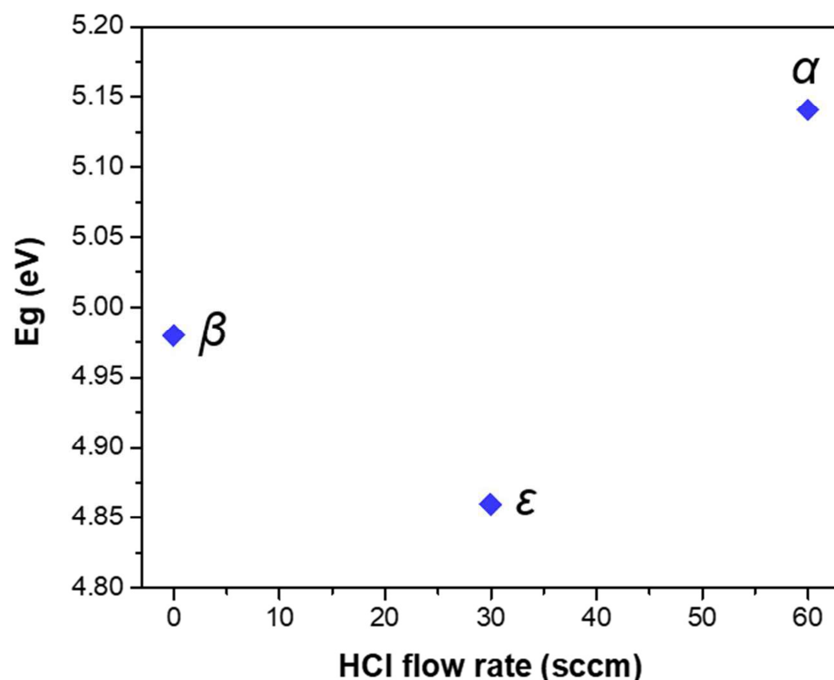

Figure 7. $(\alpha h\nu)^2$ vs. $h\nu$ plot of Ga_2O_3 films grown by different HCl flow rates.

Lastly, the transmission of the films with pure *β*- and *ε*-Ga_2O_3 and *α*-dominant Ga_2O_3 samples were collected. The spectra were converted into a Tauc plot ($(\alpha h\nu)^2$ vs. hv) where α denotes the absorption coefficient in order to determine the direct optical bandgap of the Ga_2O_3 samples. This was done by extrapolating the linear part of $(\alpha h\nu)^2$ vs. hv to the horizontal axis. As plotted in Figure 7, the band gap of the *β*-, *ε*-, and *α*-dominant Ga_2O_3 film was determined to be 4.98, 4.86, and 5.14 eV, respectively, which is consistent with the reported values for the Ga_2O_3 with different phases. [18,24,37]

CONCLUSION

Ga_2O_3 is emerging as a potential disruptive electronic material for high-voltage electronics applications. The crystal phases and orientations of MOCVD-grown Ga_2O_3 thin films on *c*-plane sapphire were investigated under different HCl flow. When the film deposited without HCl flow, (-201)-oriented *β*-Ga_2O_3 was formed. With increasing the flow of HCl to 5 sccm, the growth rate of *β*-Ga_2O_3 was tripled. With continuous increase of the HCl flow, a mixture of *β*- and *ε*-Ga_2O_3 was formed, and later transformed to pure *ε*-Ga_2O_3 when the HCl flow reached to 30 sccm

1
2
3
4
5
6
7
8
9
10
11
12
13
14
15
16
17
18
19
20
21
22
23
24
25
26
27
28
29
30
31
32
33
34
35
36
37
38
39
40
41
42
43
44
45
46
47
48
49
50
51
52
53
54
55
56
57
58
59
60

at which the film has the highest growth rate. By continuously increasing the HCl flow, the growth rate dropped while the crystal changed to a mixture of ε- and α-Ga_2O_3 but a dominant α-phase was observed for Ga_2O_3 grown at 60 sccm of HCl. The Cl concentration was similar among the investigated films. It is plausible that HCl may act as a catalyst, with the increase of HCl flow, the difference in free energy between the β-, ε and α becomes smaller, thus forming a thermally meta-stable phase, as confirmed by our DFT calculation. Essentially, the most stable β-Ga_2O_3 phase transformed into the ε-Ga_2O_3 and then the α-Ga_2O_3 after flowing 30 and 60 sccm of HCl gas, respectively. The high-resolution TEM reveals the epitaxial relationship between different phases with sapphire substrates. We believe our HCl-enhanced MOCVD process can offer a new approach to achieve low-cost, large-scale hetero-epitaxy Ga_2O_3 films for optical and power device applications.

ASSOCIATED CONTENT

Supporting Information. DFT Computational Details, TEM analysis of epitaxial relationship between ε-Ga_2O_3 and substrate, and between α- Ga_2O_3 and substrate.

AUTHOR INFORMATION

Corresponding Authors

E-mail:

*Haiding.Sun@kaust.edu.sa; ** GSTompa@structuredmaterials.com ; *** Xiaohang.Li@kaust.edu.sa

Notes

The authors declare no competing financial interest

ACKNOWLEDGEMENT AND FUNDING:

The KAUST authors would like to acknowledge the support of Baseline No. BAS/1/1664-01-01, and Equipment No. BAS/ 1/1664-01-07.

1
2
3
4
5
6
7
8
9
10
11
12
13
14
15
16
17
18
19
20
21
22
23
24
25
26
27
28
29
30
31
32
33
34
35
36
37
38
39
40
41
42
43
44
45
46
47
48
49
50
51
52
53
54
55
56
57
58
59
60

REFERENCE

[1] Sun, H.; Yin, J.; Pecora, E. F.; Dal Negro, L.; Paiella, R.; Moustakas, T. D. Deep-ultraviolet emitting AlGaN multiple quantum well graded-index separate-confinement heterostructures grown by MBE on SiC substrates *IEEE Photon. J.* **2017**, 9, 1-9

[2] Hu J.; Zhang Y.; Sun M.; Piedra D.; Chowdhury N.; Palacios T. Materials and processing issues in vertical GaN power electronics *Mater. Sci. Semicond. Process* **2017,** DOI: 10.1016/j.mssp.2017.09.033

[3] Alfaraj, N.; Mitra, S.; Wu, F.; Ajia, I. A.; Janjua, B.; Prabaswara, A.; Aljefri, R. A.; Sun, H.; Ng, T.K.; Ooi, B. S.; Roqan, I. S.; Li, X. Photoinduced entropy of InGaN/GaN pin double-heterostructure nanowires *Appl. Phys. Lett.* **2017**, 110 161110

[4] Higashiwaki, M.; Sasaki, K.; Kuramata, A.; Masui, T.; Yamakoshi, S. Gallium oxide (Ga_2O_3) metal-semiconductor field-effect transistors on single-crystal β-Ga_2O_3 (010) substrates *Appl. Phys. Lett.* **2012**, 100, 013504

[5] Pearton, S. J.; Yang, J.; Cary, P. H.; Ren, F.; Kim, J.; Tadjer, M. J.; Mastro, M. A. A review of Ga_2O_3 materials, processing, and devices *Appl. Phys. Rev.* **2018**, 5, 011301

[6] Konishi, K.; Goto, K.; Murakami, H.; Kumagai, Y.; Kuramata, A.; Yamakoshi, S.; Higashiwaki, M. 1-kV vertical Ga_2O_3 field-plated Schottky barrier diodes *Appl. Phys. Lett*. **2017**, 110, 103506

[7] Green A. J.; Chabak, K. D.; Heller, E. R.; Fitch R. C.; Baldini, M.; Fiedler, A.; Irmscher, K.; Wagner, G.; Galazka, Z.; Tetlak, S. E.; Crespo, A.; Leedy, K.; Jessen, G. H. 3.8-MV/cm Breakdown Strength of MOVPE-Grown Sn-Doped β-Ga_2O_3 MOSFETs *IEEE Electron Device Lett.* **2016**, 37, 902-905

[8] Pratiyush, A. S.; Krishnamoorthy, S.; Solanke, S. V.; Xia, Z., Muralidharan, R., Rajan, S.; Nath, D. N. High responsivity in molecular beam epitaxy grown β-Ga_2O_3 metal semiconductor metal solar blind deep-UV photodetector *Appl. Phys. Lett.* **2017**, 110, 221107

[9] Armstrong, A. M.; Crawford, M. H.; Jayawardena, A.; Ahyi, A.; Dhar, S. Role of self-trapped holes in the photoconductive gain of β-gallium oxide Schottky diodes *J. Appl. Phys*. **2016**, 119, 103102

[10] Higashiwaki, M.; Sasaki, K.; Kuramata, A.; Masui, T.; Yamakoshi, S. Development of gallium oxide power devices *Phys. Status Solidi A* **2014**, 211**,** 21-26

1 2 3 4 5 6 7 8 9 10 11 12 13 14 15 16 17 18 19 20 21 22 23 24 25 26 27 28 29 30 31 32 33 34 35 36 37 38 39 40 41 42 43 44 45 46 47 48 49 50 51 52 53 54 55 56 57 58 59 60

[11] Murakami, H.; Nomura, K.; Goto, K.; Sasaki, K.; Kawara, K.; Thieu, Q. T.; Togashi, R.; Kumagai, Y.; Higashiwaki, M.; Kuramata, A. Homoepitaxial growth of β-Ga_2O_3 layers by halide vapor phase epitaxy *Appl. Phys. Express* **2015**, 8, 015503

[12] Sasaki, K.; Kuramata, A.; Masui, T.; Víllora, E. G.; Shimamura, K.; Yamakoshi, S. Device-Quality β- Ga_2O_3 Epitaxial Films Fabricated by Ozone Molecular Beam Epitaxy *Appl. Phys. Express* **2012**, 5, 035502

[13] Rafique, S.; Han, L.; Zorman, C. A.; Zhao, H. Synthesis of Wide Bandgap β-Ga_2O_3 Rods on 3C-SiC-on-Si *Cryst. Growth Des.* **2016**, 16, 511–517

[14] Chen, Y.; Xia, X.; Liang, H.; Abbas, Q.; Liu, Y.; Du, G. Growth Pressure Controlled Nucleation Epitaxy of Pure Phase ε- and β-Ga_2O_3 Films on Al_2O_3 via Metal–Organic Chemical Vapor Deposition *Cryst. Growth Des.* **2018**, 18, 1147–1154

[15] Baldini, M.; Albrecht, M.; Fiedler, A.; Irmscher, K.; Klimm, D.; Schewski, R.; Wagner, G. Semiconducting Sn-doped β- Ga_2O_3 homoepitaxial layers grown by metal organic vapour-phase epitaxy *J. Mater. Sci.* **2016**, 51, 3650

[16] Sun, H.; Torres Castanedo, C. G.; Liu, K.; Li, K. H.; Guo, W.; Lin, R.; Liu, X.; Li, J.; Li, X. Valence and conduction band offsets of *β*-Ga2O3/AlN heterojunction *Appl. Phys. Lett.* **2017**, 111, 162105

[17] Roy, R.; Hill, V.G.; Osborn, E. F. Polymorphism of Ga_2O_3 and the System Ga_2O_3-H_2O *J. Am. Chem. Soc.* **1952**, 74, 719-722

[18] Oshima, Y.; Víllora, E. G.; Matsushita, Y.; Yamamoto, S.; Shimamura, K. Epitaxial growth of phase-pure ε- Ga_2O_3 by halide vapor phase epitaxy *J. Appl. Phys.* **2015**, 118, 085301

[19] Xia, X.; Chen, Y.; Feng, Q.; Liang, H.; Tao, P.; Xu, M.; Du, G. Hexagonal phase-pure wide band gap ε-Ga_2O_3 films grown on 6H-SiC substrates by metal organic chemical vapor deposition *Appl. Phys. Lett.* **2016**, 108**,** 202103

[20] Boschi, F.; Bosi, M.; Berzina, T.; Buffagni, E.; Ferrari, C.; Fornari, R. Hetero-epitaxy of ε-Ga_2O_3 layers by MOCVD and ALD *J. Cryst. Growth* **2016**, 443, 25-30

[21] Cora, I.; Mezzadri, F.; Boschi, F.; Bosi, M.; Čaplovičová, M.; Calestani, G.; Dódony, I.; Pécz, B.; Fornari, R. The real structure of ε- Ga_2O_3 and its relation to κ-phase *Cryst. Eng. Comm.* **2017**, 19, 1509-1516

1
2
3
4
5
6
7
8
9
10
11
12
13
14
15
16
17
18
19
20
21
22
23
24
25
26
27
28
29
30
31
32
33
34
35
36
37
38
39
40
41
42
43
44
45
46
47
48
49
50
51
52
53
54
55
56
57
58
59
60

[22] Yao, Y.; L. A. M. Lyle, J. A. Rokholt, Okur, S.; Tompa, G. S.; Salagaj, T.; Sbrockey, N.; Davis, R. F.; Porter, L. M. Growth and Characterization of α-, β-, and ε-Ga_2O_3 Epitaxial Layers on Sapphire *ECS Trans.* **2017**, 80, 191-196

[23] Playford, H. Y.; Hannon, A. C.; Barney, E. R.; Walton, R. I. Structures of Uncharacterised Polymorphs of Gallium Oxide from Total Neutron Diffraction *Chem. Eur. J.* **2013**, 19, 2803-2813

[24] Stepanov, S. I.; Nikolaev, V. I.; Bougrov, V. E.; Romanov, A. E. Gallium Oxide: Properties and Applica A Review *Rev. Adv. Mater. Sci.* **2016**, 44, 63-86

[25] Kaneko, K.; Kawanowa, H.; Ito, H.; Fujita, S. Evaluation of Misfit Relaxation in α-Ga_2O_3 Epitaxial Growth on α-Al_2O_3 Substrate *Jpn. J. Appl. Phys.* **2012**, 51, 020201

[26] Segura, A.; Artús, L.; Cuscó, R.; Goldhahn, R.; Feneberg, M. Band gap of corundumlike α-Ga_2O_3 determined by absorption and ellipsometry *Phys. Rev. Materials* **2017**, 1, 024604

[27] Kawaharamura, T.; Dang, G. T.; Furuta, M. Successful Growth of Conductive Highly Crystalline Sn-Doped α-Ga_2O_3 Thin Films by Fine-Channel Mist Chemical Vapor Deposition *Jpn. J. Appl. Phys.* **2012**, 51, 040207

[28] Cuscó, R.; Domènech-Amador, N.; Hatakeyama, T.; Yamaguchi, T.; Honda, T.; Artús, L. Lattice dynamics of a mist-chemical vapor deposition-grown corundum-like Ga_2O_3 single crystal *J. Appl. Phys.* **2015**, 117, 185706

[29] Akaiwa, K.; Kaneko, K.; Ichino, K.; Fujita, S. Conductivity control of Sn-doped α-Ga_2O_3 thin films grown on sapphire substrates *Jpn. J. Appl. Phys.* **2016**, 55, 1202BA

[30] D. Tamba, D.; Kubo, O.; Oda, M.; Osaka, S.; Takahashi, K.; Tabata, H.; Kaneko, K.; Fuijta, S.; Katayama, M. Surface termination structure of α-Ga_2O_3 film grown by mist chemical vapor deposition *Appl. Phys. Lett.* **2016**, 108, 251602

[31] Oshima, Y.; Víllora, E.G.; Shimamura, K. Halide vapor phase epitaxy of twin-free α-Ga_2O_3 on sapphire (0001) substrates *Appl. Phys. Express* **2015**, 8, 055501

[32] Schewski, R.; Wagner, G.; Baldini, M.; Gogova, D.; Galazka, Z.; Schulz, T.; Remmele, T., Markurt, T.; von Wenckstern, H.; Grundmann, M. Epitaxial stabilization of pseudomorphic α-Ga_2O_3 on sapphire (0001) *Appl. Phys. Express* **2015**, 8, 011101

[33] Ju, M. G.; Wang, X.; Liang, W.; Zhao, Y.; Li, C. Tuning the energy band-gap of crystalline gallium oxide to enhance photocatalytic water splitting: mixed-phase junctions *J. Mater. Chem. A* **2014**, 2, 17005

[34] He, H.; Orlando, R.; Blanco, M. A.; Pandey, R. First-principles study of the structural, electronic, and optical properties of Ga_2O_3 in its monoclinic and hexagonal phases *Phys. Rev. B* **2006**, 74, 195123

[35] Yoshioka, S.; Hayashi, H.; Kuwabara, A.; Oba, F.; Matsunaga, K.; Tanaka, I. Structures and energetics of Ga_2O_3 polymorphs *J. Phys.: Condens. Matter* **2007**, 19, 346211

[36] Sabino, F. P.; de Oliveira, L. N.; Da Silva, F. L. F. Role of atomic radius and d-states hybridization in the stability of the crystal structure of M_2O_3 (M = Al, Ga, In) oxides *Phys. Rev. B* **2014**, 90, 155206

[37] Chikoidze, E.; von Bardeleben, H. J.; Akaiwa, K.; Shigematsu, E.; Kaneko, K.; Fujita, S. Electrical, optical, and magnetic properties of Sn doped α-Ga_2O_3 thin films *J. Appl. Phys.* **2016**, 120, 025109

1
2
3
4
5
6
7
8
9
10
11
12
13
14
15
16
17
18
19
20
21
22
23
24
25
26
27
28
29
30
31
32
33
34
35
36
37
38
39
40
41
42
43
44
45
46
47
48
49
50
51
52
53
54
55
56
57
58
59
60

For Table of Contents Use Only (TOC)

Manuscript title: HCl Flow-induced Phase Change of *α*-, *β*- and *ε*-Ga_2O_3 Films Grown by MOCVD

Author list: *Haiding Sun[1*], Kuang-Hui Li[1], C. G. Torres. Castanedo[1], Serdal Okur[2], Gary S. Tompa[2**], Tom Salagaj[2], Sergei Lopatin[3], Alessandro Genovese[3], Xiaohang Li[1***]*

[1] King Abdullah University of Science and Technology (KAUST), Advanced Semiconductor Laboratory, Thuwal, 23955-6900, Saudi Arabia

[2] Structured Materials Industries, Inc., Piscataway, New Jersey 08854, USA

[3] King Abdullah University of Science and Technology (KAUST), Imaging and Characterization Core Laboratory, Thuwal 23955-6900, Saudi Arabia

TOC graphic, and synopsis.

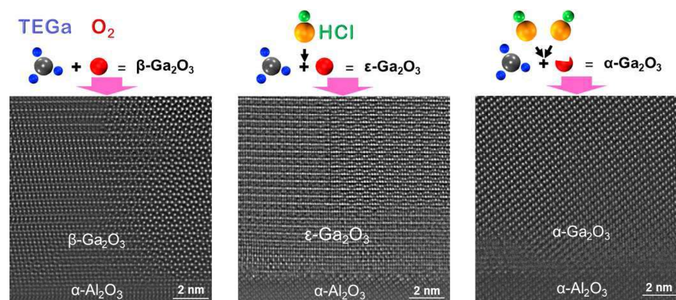

Tuning the phases of Ga_2O_3 films (*α, β* and *ε*) via HCl flow in a MOCVD reactor